Bayesian Filtering and Some Markovian Random Fields for Image Restoration

José Ismael de la Rosa, *Member, IEEE*, Jesús Villa, Efrén González, Ma. Araiza, Osvaldo Gutiérrez, Maria de la Luz Escobar, and Gilles Fleury

Abstract— **The present work introduces an alternative method to deal with digital image restoration into a Bayesian framework, particularly, the use of a new half-quadratic function is proposed. The Bayesian methodology is based on the prior knowledge of some information that allows an efficient modelling of the image acquisition process. The edge preservation of objects into the image while smoothing noise is necessary in an adequate model. Thus, we use a convexity criteria given by a semi-Huber function to obtain adequate weighting of the cost functions (half-quadratic) to be minimized. A comparison between the new introduced scheme and other three existent schemes, for the cases of noise filtering and image deblurring, is presented. Results showed a satisfactory performance and the effectiveness of the proposed estimator.**[1]

Keywords— **Image filtering, image deblurring, Markov Random Fields (MRF), Half-quadratic functions.**

I. Introduction

THE use of powerful methods proposed in the seventies under the name of Bayesian estimation [4], [5], [17], are nowadays essential at least in the cases of image filtering, segmentation and restoration (e.g. image deblurring) [2]. The basic idea of these methods is to construct a Maximum a posteriori (MAP) estimate of the modes or so called estimator of true images by using Markov Random Fields (MRF) in a Bayesian framework. The idea is based on a robust scheme which could be adapted to reject outliers, tackling situations where noise is present in different forms during the acquisition process [3], [8], [15], [16], [28], [29], [30], [33].

The image restoration or recuperation approaches of an image to its original condition given a degraded image, pass by reverting the effects caused by a distortion function. In fact, the degradation characteristics given by $F(x)$ and n in equation (1) are crucial information and they must be known or estimated during the inversion procedure. Typically, $F(x)$ is related to a point spread function H which can be linked with the probability distribution of the noise contamination n. In the case of MAP filters, usually the additive Gaussian noise is considered. A global image formulation model could be:

$$y = F(x) + n, \tag{1}$$

where $F(x)$ is a functional that could take for instance, two forms: $F(x) = x$ and $F(x) = Hx$, being H a linear operator which models the image degradation. All variables presented along the text are, x: which represents a Markov random field (or image to be estimated), y: represents the observed image with additive noise n and / or distorted by H, and $\widehat{x}$: is the estimator of x with respect to data y. There is another source of information which imposes a key rule in the image processing context, this is the spatial information that represents the likelihood or correlation between the intensity values of a neighborhood of pixels well specified. The modellig, when using MRF, takes into account such spatial interaction and it was introduced and formalized by Besag [4], where the powerfulness of these statistical tools is shown (as well as in pioneering works [5], [17], [6], [39]). Combining both kinds of information in a statistical framework, the restoration is led by an estimation procedure given the maximum a posteriori of the true images when the distortion functionals are known. The algorithms implemented in this work were developed considering a degraded signal, where the resulting non-linear recursive filters show excellent characteristics to preserve all the details contained in the image, and on the other hand, they smooth the noise components. Particularly four estimation schemes are implemented using, the semi-Huber potential function which is proposed as an extension of some previous works [13], [14] (see in section III), and the generalized Gaussian MRF introduced in the work of Bouman [6], the Welch and Tukey potential functions as used in the works of Rivera [35], [36], [37] (see in section IV).

Section II describes the general definition of MAP estimator and MRFs. The potential functions compared in this paper must be obtained or proposed to conduct adequately the inversion process. Such functions are described in sections III and IV where the convexity is the key to formulate an adequate criterion to be minimized. In sections V and VI, the MAP estimators resulting from different MRF structures and some illustrative results are briefly discussed. Finally, in section VII some partial conclusions and comments are given.

II. MAP estimation and Markov random fields

The problem of image estimation (e.g. filtering or restoration) into a Bayesian framework deals with the solution of an inverse problem, where the estimation process is carried out in a whole stochastic environment. The most popular estimators used nowadays are:

Maximum Likelihood (ML) estimator:

$$\widehat{x}_{\mathbf{ML}} = \arg\max_{x \in \mathbf{X}} p(y|x), \tag{2}$$

Corresponding autor, e-mail:ismaelrv@ieee.org

[1]The authors work at Universidad Autónoma de Zacatecas - Unidad Académica de Ingeniería Eléctrica, Lab. de Procesamiento Digital de Señales, Av. López Velarde No. 801, Col. Centro, C.P. 98068, Zacatecas, Zacatecas, Mexico.

ISBN: 978-607-95476-3-9

this estimator is a classical approach i
In a probabilistic framework, the regularization of the ML estimator leads to the Bayesian approach, where it is important to exploit all known information or so called prior information about any process under study, which gives a better statistical estimator called
Maximum A Posteriori (MAP) estimator:

$$\begin{aligned}\widehat{x}_{\mathbf{MAP}} &= \arg\max_{x\in\mathbf{X}} p(x|y) \\ &= \arg\max_{x\in\mathbf{X}} \left(\log p(y|x) + \log g(x)\right),\end{aligned} \tag{3}$$

in this case, the estimator is regularized by using a Markov random field function $g(x)$ which models all prior information as a whole probability distribution, where $\mathbf{X}$ is the set of pixels x capable to maximize $p(x|y)$, and $p(y|x)$ is the likelihood probability function from y given x.
The Markov random fields (MRF) can be represented in a general way by using the following equation:

$$g(x) = \frac{1}{Z}\exp\left(-\sum_{c\in\mathbf{C}} V_c(x)\right), \tag{4}$$

where Z is a normalization constant, $\mathbf{C}$ is a set of "cliques" c or local neighborhoods of pixels, and $V_c(x)$ is a weighting function given over the local group of points c. Generally, the "cliques" correspond to the sets of neighborhoods of pixels if $\forall s, r \in c$, s and r are neighbors, and one can construct a neighborhood system called ∂s; for the 8 closest neighbors $\partial s = \{r : |s-r| < 2\}$. The Markov random fields have the capacity to represent various image sources.

There is a variety of MRF models which depend on the cost functions also known as potential functions that can be used. Each potential function characterizes the interactions between pixels in the same local group. As an example, the following family represents convex functions:

$$\rho(\Delta) = |\Delta|^p \tag{5}$$

where $\Delta = \lambda[x_s - x_r]$, λ is a constant parameter to be chosen, and p takes constant values such as $p \geq 1$ accordingly to the theorem 2 in [6].

III. Semi-Huber (SH) proposed potential function

The principal apport of this work is the proposition of the semi-Huber potential for image restoration, which performance is comparable with respect to half-quadratic functionals performance. In order to assure completely the robustness into the edge preserving image filtering, diminishing at the same time the convergence speed, the Huber–like norm or semi–Huber (SH) potential function is proposed as a half-quadratic (HQ) function. Such functional has been used in one dimensional robust estimation as described in [13] for the case of non-linear regression. This function is adjusted in this work in two dimensions according to the following equation:

$$\log g(x) = -\lambda\left(\sum_{\{s,r\}\in\mathbf{C}} b_{sr}\rho_1(x)\right) + \text{ct}, \tag{6}$$

$$\rho_1(x) = \frac{\Delta_0^2}{2}\left(\sqrt{1+\frac{4\varphi_1(x)}{\Delta_0^2}} - 1\right),$$

and where $\Delta_0 > 0$ is a constant value, b_{sr} is a constant that depends on the distance between the r and s pixels, ct is a constant term, and $\varphi_1(x) = e^2$ where $e = (x_s - x_r)$. The potential function $\rho_1(x)$ fulfills the following conditions

$$\begin{aligned}\rho_1(x) &\geq 0, && \forall x \quad \text{with } \rho_1(0) = 0, \\ \psi(x) &\equiv \partial\rho_1(x)/\partial x, && \text{exists}, \\ \rho_1(x) &= \rho_1(-x), && \text{is symmetric}, \\ w(x) &\equiv \tfrac{\psi(x)}{2x}, && \text{exists}, \\ \lim_{x\to+\infty} w(x) &= \mu, && 0 \leq \mu < +\infty, \\ \lim_{x\to+0} w(x) &= M, && 0 < M < +\infty.\end{aligned} \tag{7}$$

Figure 1(a) shows the behavior of the semi-Huber proposed function for different Δ_0 values, in the range of $x \in [-8, 8]$. Notice that there is not necessary a scale parameter and that the potential function meets all requirements imposed by conditions (7).

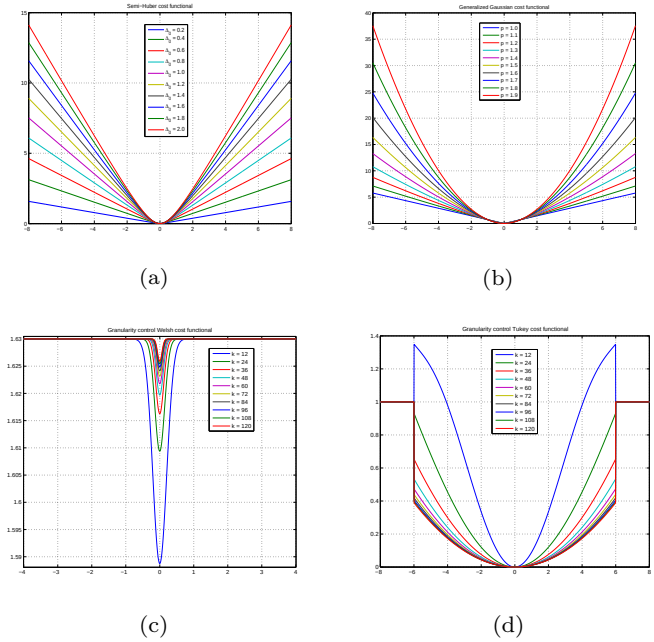

(a) (b) (c) (d)

Fig. 1. The four convex potential functions used: (a) The Semi-Huber potential function for Δ_0 with different values; (b) The Generalized Gaussian potential function for p different values, while $q = 2$; (c) The granularity control Welch potential function for k different values, while $\mu = 0.01$; (d) The granularity control Tukey potential function for k different values, while $\mu = 0.01$.

IV. Generalized Gaussian MRF and other half-quadratic functions

In some works [7], [10], [11], [21], [22] a variety of new potential functions were introduced, such proposed functions are semi-quadratic functionals or half-quadratic and they characterize certain convexity into the regularization term [18], [19](eg. extension of penalization) which permits to build efficient and robust estimators in the sense of data preservation which is linked to the original or source image. Also, the necessary time of computation decreases

ISBN: 978-607-95476-3-9

with respect to other proposed schem*nction* Nikolova [8], [15], [16], [28], [29], [30], [31] and Labat [23], [24]. On the other hand, a way to obtain the posterior distribution of images has been proposed in previous works from A. Gibbs [20], in this case, it is necessary to use sophisticated stochastic simulation techniques based on the Markov Chain Monte Carlo (MCMC) methods [27], [38]. If it is possible to obtain the posterior distribution of any image, then, it is also possible to sample from such posterior distribution to obtain the MAP estimator, or other estimators such as the median estimator. The MAP and the median estimators search the principal mode of the posterior distribution.

In the present paper some potential functions are compared. The proposed semi-Huber is compared with respect to the generalized Guassian MRF introduced in [6], [39], the Welch, and Tukey potential functions with granularity control. These two last functions were proposed and used in recent works [35], [36], [37] proving excellent performance.

A. Generalized Gaussian MRF (GGMRF)

If one considers to generalize the Gaussian MRF (when $p = q = 2$ one has a GMRF, see equation (15)) as proposed in [6], then the generalized potential functions can be limited such as

$$\rho_2(\Delta) = |\Delta|^p \,, \quad \text{for } 1 \le p \le 2, \tag{8}$$

obtaining the GGMRF

$$\log g(x) = -\lambda^p \left(\sum_{s\in\mathbf{S}} a_s x_s^p + \sum_{\{s,r\}\in\mathbf{C}} b_{sr}|x_s - x_r|^p \right) + \text{ct}, \tag{9}$$

where theoretically $a_s > 0$ and $b_{sr} > 0$, s is the site or pixel of interest and $\mathbf{S}$ is the set of sites into the whole MRF, and r corresponds to the local neighbors. In practice it is recommended to take $a_s = 0$ thus, the unicity of $\widehat{x}_{\mathbf{MAP}}$, can be assured given that the likelihood term is quadratic $q = 2$, then

$$\log g(x) = -\lambda^p \left(\sum_{\{s,r\}\in\mathbf{C}} b_{sr}|x_s - x_r|^p \right) + \text{ct}, \tag{10}$$

and from equation (3), $\log p(y|x)$ is strictly convex and so $\widehat{x}_{\mathbf{MAP}}$ is continuous in y, and in p. The choice of the power p is capital, since it constrains the convergence speed of the local or global estimator, and the quality of the restored image. Small values for p allows abrupt discontinuities modeling while large values smooth them. Figure 1(b) shows the behavior of the generalized Gaussian function for different p values, in the range of $x \in [-8, 8]$. The proposition of such function avoids the use of a scale parameter and at the same time the potential function meets all requirements imposed by conditions (7).

Known as a hard redescender potential function with granularity control given by μ, and proposed in [35]

$$\log g(x) = -\lambda \left(\mu \sum_{\{s,r\}\in\mathbf{C}} b_{sr}\varphi_1(x) + (1-\mu) \sum_{\{s,r\}\in\mathbf{C}} b_{sr}\rho_3(x) \right) + \text{ct}, \tag{11}$$

where k is a positive scale parameter and

$$\rho_3(x) = 1 - \frac{1}{2k}\exp(-k\varphi_1(x)).$$

This function is also half-quadratic such as the Tukey function presented in the following subsection. Figure 1(c) shows the behavior of the Welsh function with granularity control for different k threshold values, in the range of $x \in [-8, 8]$, $\mu = 0.01$. Also, this potential function fulfills all requirements imposed by conditions (7).

C. Tukey MRF function

This is another hard redescender potential function, proposed in [35] that fulfills all requirements imposed by conditions (7)

$$\log g(x) = -\lambda \left(\mu \sum_{\{s,r\}\in\mathbf{C}} b_{sr}\varphi_1(x) + (1-\mu) \sum_{\{s,r\}\in\mathbf{C}} b_{sr}\rho_4(x) \right) + \text{ct}, \tag{12}$$

where

$$\rho_4(x) = \begin{cases} 1 - (1 - (2e/k)^2)^3, & \text{for } |e/k| < 1/2, \\ 1, & \text{otherwise.} \end{cases}$$

and where k is also a scale parameter. On the other hand, $\varphi_1(x)$ can be the quadratic function which together with μ induces the granularity control. Figure 1(d) shows the behavior of the Tukey function with granularity control for different k values, in the range of $x \in [-8, 8]$, $\mu = 0.01$.

V. MAP estimators and practical convergence

A. Image filtering

In this section some estimators are deduced. The single problem of filtering noise to restore an observed signal y leads to establish the estimators. The observation equation could be

$$y = x + n, \text{ where } n \sim \mathcal{N}(0, I\sigma_n^2),$$

where I is the identity matrix, and where the general MAP estimator for this case is deduced from the next minimization process

$$\widehat{x}_{\mathbf{MAP}} = \arg\min_{x\in\mathbf{X}} \left(-\log p(y|x) - \log g(x) \right). \tag{13}$$

ISBN: 978-607-95476-3-9

Thus, under hypothesis of Gaussian no H is known and given by the following truncated Gaussian blurring function,

$$h(i,j) = \exp\left(\frac{-i^2-j^2}{2\sigma_b^2}\right), \text{ for } -3 \leq i,j \leq 3, \quad (18)$$

as used also in [32], with $\sigma_b = 1.5$. And $k = 1,2,3,4$ according to the four SH, GGMRF, Welsh and Tukey potential functions. Here, the results were improved combining ideas introduced in a similar Bayesian way by Levin [25], [26] adding a Sparse prior (SP) for filtering and then reconstructing the image.

$$\widehat{x}_{\mathbf{MAP_k}} = \arg\min_{x\in\mathbf{X}} \left(\sum_{s\in\mathbf{S}} |y_s - x_s|^2 - \log g(x) \right), \quad (14)$$

where $k = 1,2,3,4$ according to the four SH, GGMRF, Welsh and Tukey potential functions, and assuming homogeneity of the MRFs. On the other hand, the minimization problem leads to consider various methods [1], [8], [9], [28], [29], [30], [31]:

- global iterative techniques such as: the descendent gradient [31], conjugate gradient [35] (for recent propositions one can consult the work [23], [24]), Gauss-Seidel, Over-relaxed methods, etc.
- local minimization techniques: minimization at each pixel x_s (which generally needs more time, but from our point of view are more precise), where also some of the above methods can be used.

In this work the local techniques were used (the expectation maximization (EM) could also be implemented, or the complete half-quadratic scheme as proposed by Geman and Reinolds [18], and Geman and Yang [19]), since all hyper-parameters included into the potential functions were chosen heuristically or according to values proposed in references. Only, the step of minimization with respect to x was implemented to probe convergence of estimators. For instance, the local MAP2 estimator for the GGMRF is given by

$$\widehat{x}_s = \arg\min_{x_s\in\mathbf{X}} \left\{ |y_s - x_s|^q + \sigma^q \lambda^p \sum_{r\in\partial\mathbf{s}} b_{r-s} |x_s - x_r|^p \right\}. \quad (15)$$

For intermediate values of p and q the estimators become sub-optimal, and the iterated methods can be used to minimize the obtained criterions. Some iterative methods are the sub–gradient, and the Levenberg–Marquardt method of MATLAB 7, the last was used in this work [12]. For cases where $q \neq p$, for example $q = 2$ and $1 < p < 2$, some studies and different prior functions have been proposed in [15], [16], [28], [29], [30], [31], particulary in [15], [16], [28], [30] where non-convex regularized least-squares schemes are deduced and its convergence is analyzed (where $0 < p < 1$) with very good times of convergence as presented in [32].

B. Image deconvolution

On the other hand, for the problem of image deblurring to restore an observed signal y, the observation equation used is given by

$$y = Hx + n, \text{ with } n \sim \mathcal{N}(0, I\sigma_n^2). \quad (16)$$

Now, for the four MAP estimators the likelihood term changes, such that,

$$\widehat{x}_{\mathbf{MAP_k}} = \arg\min_{x\in\mathbf{X}} \left\{ \sum_{s\in\mathbf{S}} |y_s - Hx_s|^2 - \log g(x) \right\}, \quad (17)$$

VI. Some experiments

Results presented in this section were concerned experimenting extensively with five images: synthetic, Lena, Cameraman, Boat and fringe pattern, to probe the performance of the presented estimators.

A. Image filtering

Continuing with the problem of filtering noise, some estimation results are presented when images are contaminated by Gaussian noise, and there are no other type of distortions. The first experiment was made considering that $\sigma_n = 5, 10, 15$. Different levels of noise were added to the images: $n \sim \mathcal{N}(0, I\sigma_n^2)$, the values of σ_n are given such that the obtained degradation is perceptible and difficult to eliminate. The results were compared using different values for Δ_0 and with $\lambda = 1$ (MAP1), different values for p and λ preserving $q = 2$ (MAP2), and different values for k, μ and λ (MAP3 and MAP4). Generally, with the four estimators the filtering task gives good visual results (see Figures 2 and 3), but the time of computation is different between them, the fastest estimator is the MAP3, while the slowest is the MAP2 with $p = 1.2$ which results correspond to the Cameraman in Figure 2 (d). In the case of the Welsh and Tukey functionals the tuning problems must be solved implementing in correct ways more sophisticated algorithms based on the expectation maximization method. In Figure 3 a synthetic generated fringe pattern image was also used to probe performance of estimators. In this case, it is known how is the noise structure that contaminates data, but the signal-to-noise is unknown. Clearly, once again the results obtained coincide with the previous results for other images, but with an increase of time of computation which has a relation with the image dimensions (as shown in Table I). Some interesting applications of robust estimation are particulary focused in phase recovery from fringe patterns as presented in a recent work [40], phase unwrapping, and some other problems in optical instrumentation, in this sense some filtering results were thus obtained using the presented MAP estimators.

Finally, Table I shows the performance of the four MAP estimators for the problem of filtering Gaussian noise, where an objective evaluation is conducted accordingly to the pique signal to noise ratio (PSNR). Also the computation times in MATLAB are shown in Table I. Such comparative evaluation shows that our proposed approach

ISBN: 978-607-95476-3-9

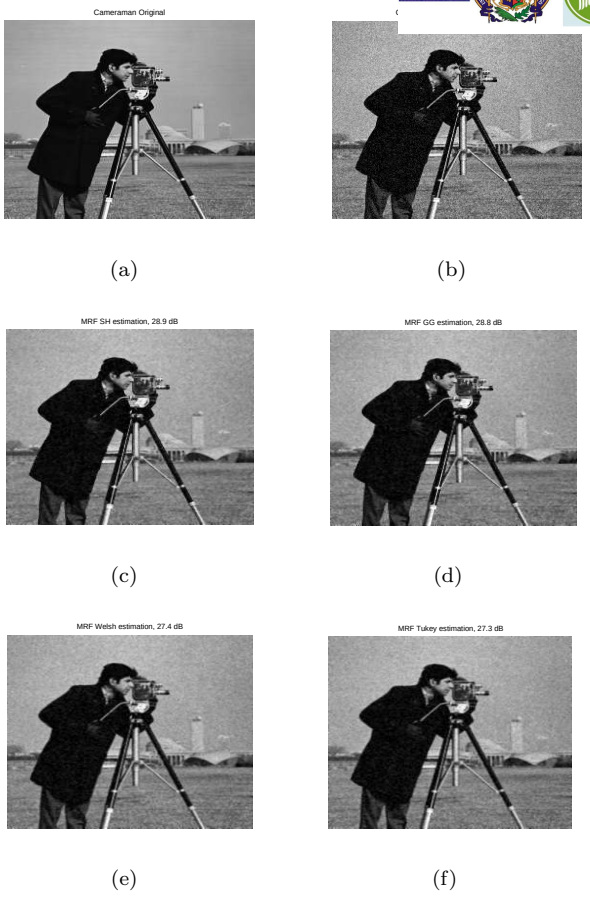

Fig. 2. Results for Cameraman standard image: (a) describes the original image; (b) describes the noisy image using Gaussian noise with $\sigma_n = 15$; (c) filtered image using MAP1 ($\Delta_0 = 20$); (d) filtered image using MAP2 ($\lambda = 30$, $p = 1.2$); (c) filtered image using MAP3 ($k = 2000$, $\mu = 0.025$, $\lambda = 30$); (d) filtered image using MAP4 ($k = 2000$, $\mu = 0.025$, $\lambda = 30$).

MAP1, gives better or similar performance with respect to MAP2, MAP3, and MAP4. On the other hand, the use of

TABLE I

RESULTS OBTAINED IN EVALUATING THE FILTERING CAPACITY OF THE DIFFERENT MAP ESTIMATORS USING FOUR IMAGES.

\	$\sigma_n = 15$	MAP1	MAP2	MAP3	MAP4
synthetic	PSNR	24.7	24.6	24.7	24.6
35×35	PSNR filt.	28.8	27.6	25.5	25.6
	Time (sec)	5.9	7.6	4.6	5.2
Lena	PSNR	24.5	24.5	24.6	24.6
120×120	PSNR filt.	29.1	28.9	26.0	27.5
	Time (sec)	75.3	80.6	59.9	59.1
Cameraman	PSNR	24.6	24.7	24.6	24.6
256×256	PSNR filt.	28.9	28.8	27.3	27.4
	Time (sec)	341.7	355.9	243.8	243.6
Boat	PSNR	24.6	24.6	24.6	24.6
512×512	PSNR filt.	29.4	29.5	27.3	28.8
	Time (sec)	1,243.3	1,545.5	1,014.2	1,051.4

half-quadratic potential functions permits flexibility on the computation times [15], [16], [30], but still is a challenge to tune correctly the hyper-parameters to obtain a better performance in the sense of quality restoration. Perhaps the most simple potential function to tune is the semi-Huber (MAP1). Also, making the correct hypothesis over the noise could help to improve the performance of the estimator. This could be directly reflected by proposing a more adapted likelihood function, as proposed in [3] and some other recent works [28] (in cases of non-Gaussian noise), where a connection with variational and partial differential equations is illustrated evoking the famous work of Perona and Malik [34], and some recent related works.

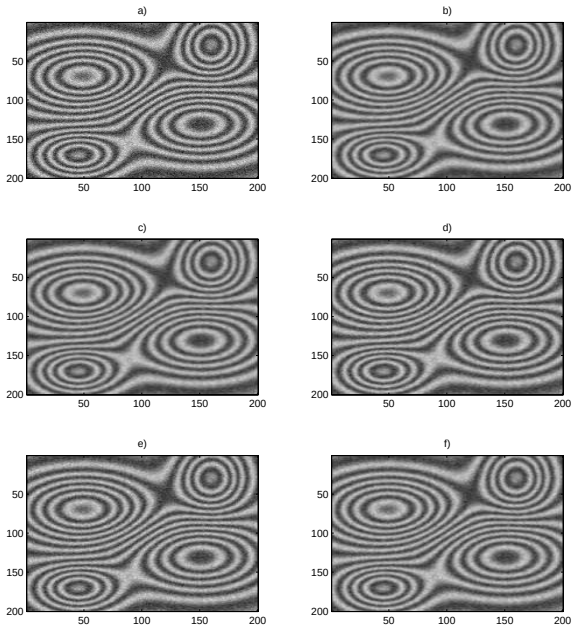

Fig. 3. a) Image with Gaussian noise with unknown σ_n (200×200), b) MAP2 estimation, $p = 1.5$ (100 s), c) MAP2 estimation, $p = 1.2$ (120 s), d) MAP1 estimation (52 s), e) MAP3 estimation (50 s) and f) MAP4 estimation (52 s).

B. Image deconvolution

Now, for the problem of image deconvolution some estimation results are presented when images are contaminated by Gaussian noise, and Gaussian distortion (with $\sigma_b = 1.5$) blurring the image. This second experiment was made considering that $\sigma_n = 3, 5, 7$. The results were compared using different values for Δ_0 and with $\lambda = 1$ (MAP1), different values for p and λ preserving $q = 2$ (MAP2), and different values for k, μ and λ (MAP3 and MAP4). Figure 4 shows a comparison of results obtained for the Cameraman image accordingly to the four MAP estimators. One can notice that preserving values of hyper-parameters near those used for the filtering case, the estimators smooth the noise but does not made a good recuperation of the image. One must change the hyper-parameter values searching a trade of between the granularity of the noise and the sharpness of the image. In Figure 5 the results obtained on the Cameraman image using a combination of proposed estimators

ISBN: 978-607-95476-3-9

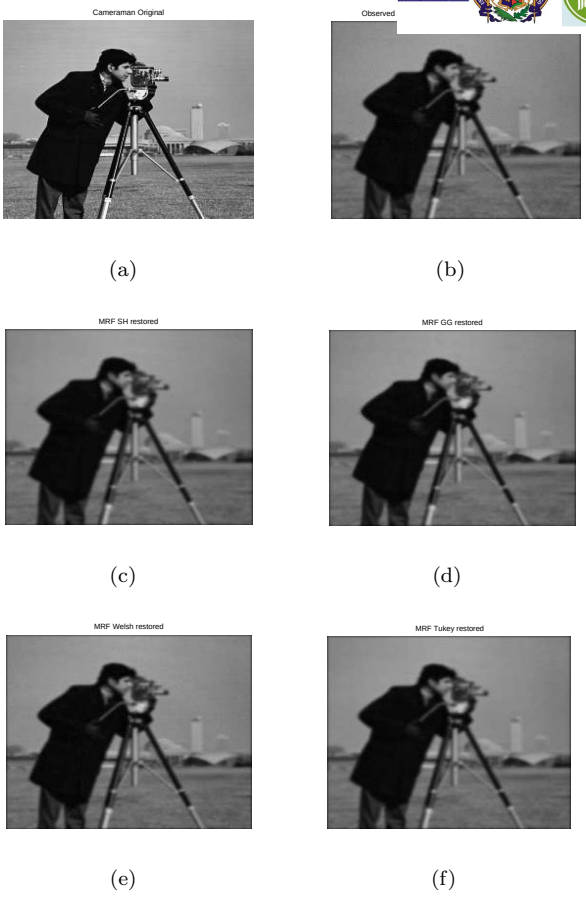

Fig. 4. Results for Cameraman standard image: (a) describes the original image; (b) describes the distorted image using Gaussian noise with $\sigma_n = 3$; (c) restored image using MAP1 ($\Delta_0 = 20$); (d) restored image using MAP2 ($\lambda = 30$, $p = 1.2$); (c) restored image using MAP3 ($k = 2000$, $\mu = 0.0015$, $\lambda = 10$); (d) restored image using MAP4 ($k = 2000$, $\mu = 0.0015$, $\lambda = 10$).

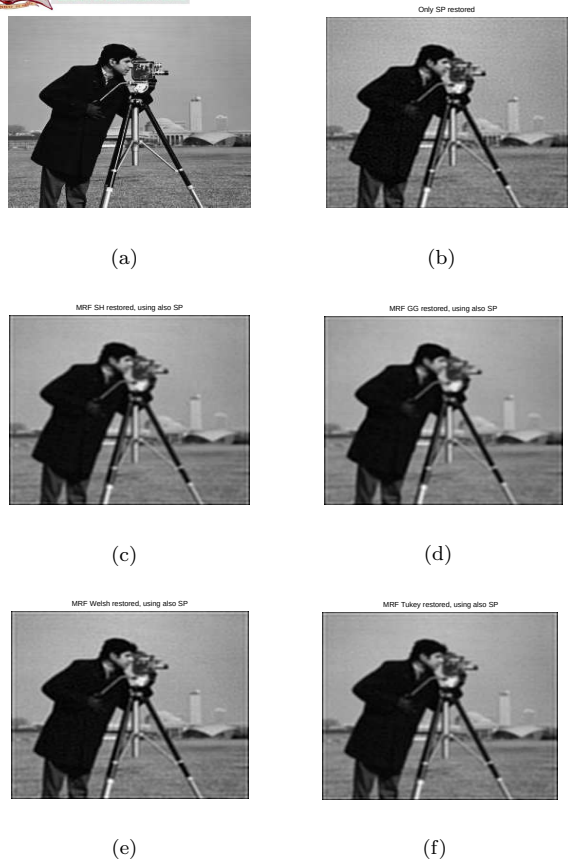

Fig. 5. Results for Cameraman standard image: (a) describes the original image; (b) describes restored image using only a Sparse prior (SP) deconvolution technique [25]; (c) restored image using MAP1 and SP ($\Delta_0 = 20$); (d) restored image using MAP2 and SP ($\lambda = 0.15$, $p = 1.2$); (c) restored image using MAP3 and SP ($k = 2000$, $\mu = 0.0015$, $\lambda = 10$); (d) restored image using MAP4 and SP ($k = 2000$, $\mu = 0.0015$, $\lambda = 10$).

together with a Sparse prior (SP) deconvolution technique introduced in [25], [26], are shown, the improvement in restoration is visible. Also, in Table II the performance of the four MAP estimators and the SP deconvolution is shown, where an objective evaluation is made accordingly to the PSNR and also times of calculation in MATLAB are shown. Here also the approach MAP1, gives similar performance with respect to MAP2, MAP3, and MAP4.

TABLE II

Results obtained in evaluating the deconvolution capacity of the different MAP estimators using three images.

$\diagdown$	$\sigma_n = 3$	MAP1	MAP2	MAP3	MAP4
Lena	PSNR	17.4	17.4	17.4	17.4
120×120	PSNR rest.	17.5	17.6	17.4	17.3
	PSNR rest. SP	20.8	20.8	20.8	20.4
	Time (sec)	58.9	91.3	58.8	59.2
Cameraman	PSNR	19.3	19.3	19.3	19.3
256×256	PSNR rest.	19.4	19.4	19.4	19.3
	PSNR rest. SP	22.5	22.3	22.5	22.2
	Time (sec)	257.7	408.0	256.8	256.9
Boat	PSNR	20.4	20.4	20.4	20.4
512×512	PSNR rest.	20.5	20.5	20.4	20.4
	PSNR rest. SP	25.6	25.8	26.0	25.9
	Time (sec)	1,014.9	1,606.5	1,011.8	1,017.5

VII. Conclusions and comments

The use of prior distribution functions based on the logarithm, with any degree of convexity and quasi-homogeneous, permits to consider a variety of possible choices of potential functions. Maybe, the most important challenges that must be well solved are: the adequate selection of hyper-parameters from potential functions, where different versions of the EM algorithms try to tackle this problem. Another is the minimization procedure which in any sense will regulate the convergence speed as proposed in [1], [18], [19], [35], [23], [24], and [28], [29], [31].

In the case of the semi-Huber potential function, the tuning is less complicated and of course, the estimator manipulation is far simpler than the Welsh and Tukey. However, this problem can be solved as argued by Idier [7] and Rivera [35] by implementing more sophisticated algorithms with the compromise to reduce time of computation and better quality in restoration as recently exposed in [9], [32], [33]. The final objective of this work has been to contribute with a series of software tools for image analysis focused for instance to optical instrumentation tasks such

ISBN: 978-607-95476-3-9

as those treated in the works [40] and [illegible] half-quadratic criteria and interacting auxiliary variables for image restoration," *IEEE Trans. on Image Processing*, Vol. 10, no. 7, pp. 1001–1009, July 2001.

competitive results in filtering and reconstruction.

References

[1] M. Allain, J. Idier, and Y. Goussard, "On global and local convergence of half-quadratic algorithms," *IEEE Trans. Image Processing*, Vol. 15, no. 5, pp. 1130–1142, may 2006.

[2] H. C. Andrews, and B. R. Hunt, *Digital image restoration*, New Jersey, Prentice-Hall, Inc., 1977.

[3] N. Bertaux, Y. Frauel, P. Réfrégier, and B. Javidi, "Speckle removal using a maximum-likelihood technique with isoline gray-level regularization," *J. Opt. Soc. Am. A*, Vol. 21, no. 12, pp. 2283–2291, 2004.

[4] J. E. Besag, "Spatial interaction and the statistical analysis of lattice systems," *J. Royal Stat. Soc. Ser. B*, Vol. B-36, pp. 192–236, 1974.

[5] J. E. Besag, "On the statistical analysis of dirty pictures," *J. Royal Stat. Soc. Ser. B*, Vol. B-48, pp. 259–302, 1986.

[6] C. Bouman, and K. Sauer, "A generalizaed Gaussian image model for edge-preserving MAP estimation," *IEEE Trans. on Image Processing*, Vol. 2, no. 3, pp. 296–310, July 1993.

[7] K. Champagnat, and J. Idier, "A conection between half-quadratic criteria and EM algorithms," *IEEE Signal Processing Letters*, Vol. 11, no. 9, pp. 709–712, Sept. 2004.

[8] T. F. Chan, S. Esedoglu, and M. Nikolova, "Algorithms for finding global minimizers of image segmentation and denoising models," *SIAM J. on Applied Mathematics*, Vol. 6, no. 5, pp. 1632–1648, 2006.

[9] E. Chouzenoux, J. Idier, and S. Moussaoui, "A majorize-minimize strategy for subspace optimization applied to image restoration," *IEEE Trans. on Image Processing*, Vol. 20, no. 6, pp. 1517–1528, Jun. 2011.

[10] P. Ciuciu, and J. Idier, "A half-quadratic block-coordinate descent method for spectral estimation," *Journal of Signal Processing*, Vol. 82, pp. 941–959, 2002.

[11] P. Ciuciu, J. Idier, and J.-F. Giovannelli, "Regularized estimation of mixed spectra using circular Gibbs-Markov model," *IEEE Trans. on Signal Processing*, Vol. 49, no. 10, pp. 2202–2213, Oct. 2001.

[12] H. F. De Campos Velho, F. M. Ramos, E. S. Chalhoub, S. Stephany, J. C. Carvalho, and F. L. De Sousa, "Inverse problems in space science and technology," *Inverse Problems in Science and Engineering*, Vol. 15, no. 4, pp. 359–372, June 2007.

[13] J. I. De la Rosa, and G. Fleury, "Bootstrap methods for a measurement estimation problem," *IEEE Trans. Instrum. Meas.*, Vol. 55, no. 3, pp. 820–827, June 2006.

[14] J. I. De la Rosa, J. J. Villa, and Ma. A. Araiza, "Markovian random fields and comparison between different convex criteria optimization in image restoration," *Proc. XVII International Conference on Electronics, Communications, and Computers - CONIELECOMP'07*, Cholula, Puebla, Mexico, February 2007.

[15] S. Durand, and M. Nikolova, "Stability of the minimizers of least squares with a non-convex regularization. Part I: Local behavior," *Journal of Applied Mathematics and Optimization*, Vol. 53, no. 2, pp. 185–208, March 2006.

[16] S. Durand, and M. Nikolova, "Stability of the minimizers of least squares with a non-convex regularization. Part II: Global behavior," *Journal of Applied Mathematics and Optimization*, Vol. 53, no. 3, pp. 259–277, May 2006.

[17] S. Geman, and D. Geman, "Stochastic relaxation, Gibbs distribution, and the Bayesian restoration of images," *IEEE Trans. Pattern Anal. Machine Intell.*, Vol. PAMI-6, pp. 721–741, Nov. 1984.

[18] D. Geman, and G. Reinolds, "Constrained restoration and the recovery of discontinuities," *IEEE Trans. Pattern Anal. Machine Intell.*, Vol. 14, no. 3, pp. 367–383, Mar. 1992.

[19] D. Geman, and C. Yang, "Nonlinear image recovery with half-quadratic regularization," *IEEE Trans. Image Processing*, Vol. 4, no. 7, pp. 932–946, July 1995.

[20] A. L. Gibbs, *Convergence of Markov Chain Monte Carlo algorithms with applications to image restoration*, Ph.D. Thesis, Department of Statistics, University of Toronto, `URL : www.utstat.toronto.edu`, 2000.

[21] J.-F. Giovannelli, J. Idier, R. Boubertakh, and A. Herment, "Unsupervised frequency tracking beyond the Nyquist frequency using Markov chains," *IEEE Trans. on Signal Processing*, Vol. 50, no. 12, pp. 2905–2914, Dec. 2002.

[23] C. Labat, and J. Idier, "Convergence of truncated half-quadratic algorithms using conjugate gradient," *technical repport*, IRCCyN, Aug. 2006.

[24] C. Labat, *Algorithmes d 'optimisation de critères pénalisés pour la restauration d 'images. Application à la déconvolution de trains d 'impulsions en imagerie ultrasonore*, Ph.D. Thesis, École Centrale de Nantes, Nantes, Dec. 2006.

[25] A. Levin, R. Fergus, F. Durand, and W. T. Freeman, "Image and depth from a conventional camera with a coded aperture," Massachusetts Institute of Technology, Computer Science and Artificial Intelligence Laboratory, SIGGRAPH, *ACM Transactions on Graphics*, Aug. 2007.

[26] A. Levin, R. Fergus, F. Durand, and W. T. Freeman, "Deconvolution using natural image priors," Massachusetts Institute of Technology, Computer Science and Artificial Intelligence Laboratory, SIGGRAPH (2007).

[27] R. M. Neal, "Probabilistic inference using Markov chain Monte Carlo methods," Tech. Rep., CRG-TR-93-1, Department of Computer Science, University of Toronto, `URL : www.cs.toronto.edu/∼radford`, 1993.

[28] M. Nikolova, *Functionals for signal and image reconstruction: properties of their minimizers and applications*, Research report to obtain the Habilitation à diriger des recherches, 2006.

[29] M. Nikolova, "Analysis of the recovery of edges in images and signals by minimizing nonconvex regularized least-squares," *SIAM Journal on Multiscale Modeling and Simulation*, Vol. 4, no. 3, pp. 960–991, 2005.

[30] M. Nikolova, and M. Ng, "Analysis of half-quadratic minimization methods for signal and image recovery," *SIAM Journal on Scientific computing*, Vol. 27, no. 3, pp. 937–966, 2005.

[31] M. Nikolova, and R. Chan, "The equivalence of half-quadratic minimization and the gradient linearization iteration," *IEEE Trans. on Image Processing*, Vol. 16, no. 6, pp. 1623–1627, 2007.

[32] M. Nikolova, M. K. Ng, and C.-P. Tam, "Fast nonconvex nonsmooth minimization methods for image restoration and reconstruction," *IEEE Trans. on Image Processing*, Vol. 19, no. 12, pp. 3073–3088, Dec. 2010.

[33] R. Pan, and S. J. Reeves, "Efficent Huber-Markov edge-preserving image restoration," *IEEE Trans. on Image Processing*, Vol. 15, no. 12, pp. 3728–3735, Dec. 2006.

[34] P. Perona, and J. Malik, "Scale-space and edge detection using anisotropic diffusion," *IEEE Trans. Pattern Anal. Machine Intell.*, Vol. 12, no. 7, pp. 629–639, July 1990.

[35] M. Rivera, and J. L. Marroquin, "Efficent half-quadratic regularization with granularity control," *Image and Vision Computing*, Vol. 21, no. 4, pp. 345–357, 2003.

[36] M. Rivera, and J. L. Marroquin, "Half-quadratic cost functions for phase unwrapping," *Optics Letters*, Vol. 29, no. 5, pp. 504–506, 2004.

[37] M. Rivera, "Robust phase demodulation of interferograms with open or closed fringes," *J. Opt. Soc. Am. A*, Vol. 22, no. 6, pp. 1170–1175, 2005.

[38] C. P. Robert, and G. Casella, *Monte Carlo Statistical Methods*, Springer Verlag, 2nd Edition, 2004.

[39] K. Sauer, and C. Bouman, "Bayesian estimation of transmission tomograms using segmentation based optimization," *IEEE Trans. on Nuclear Science*, Vol. 39, no. 4, pp. 1144–1152, 1992.

[40] J. J. Villa, J. I. De la Rosa, G. Miramontes, and J. A. Quiroga, "Phase recovery from a single fringe pattern using an orientational vector field regularized estimator," *J. Opt. Soc. Am. A*, Vol. 22, no. 12, pp. 2766–2773, 2005.

ISBN: 978-607-95476-3-9